Structural Eng./Earthquake Eng., JSCE, Vol. 15, No. 2, 215s—223s, 1998 October

CHARACTERISTICS OF INSTABILITY OF LOCAL VIBRATION OF THE THIN-WALLED MEMBERS UNDER PERIODIC AXIAL FORCES

Miyoshi OKAMURA[1] and Yasuharu FUKASAWA[2]

[1]Member of JSCE, M. Eng., Research associate, Dept. of Civil and Environmental Eng., Yamanashi University
(Takeda 4-3-11, Kofu, Yamanashi 400-8511, Japan)
[2]Member of JSCE, Dr. Eng., Professor, Dept. of Civil and Environmental Eng., Yamanashi University
(Takeda 4-3-11, Kofu, Yamanashi 400-8511, Japan)

The dynamic instability of local vibration of hinged thin-walled members under periodic axial forces is investigated by applying the finite strip method. Firstly, local buckling and free vibration of the members are analyzed and their characteristics are discussed. Secondly, the regions of instability of local vibration of the members under various geometrical parameters are calculated and the effects of some factors which control the dynamic instability phenomena are clarified. Based on the results, the most efficient arrangements of diaphragm or stiffener are described.

Key Words : *thin-walled member, dynamic local instability, local buckling, finite strip method*

1. INTRODUCTION

When thin-walled members of a steel truss structure are subjected to dynamic load, periodic axial stresses are generated. In such members, not only overall member bending vibrations but also out-of-plane bending vibrations in component plates of a thin-walled member are generated as parametric resonance vibration. These local vibrations in the members of a truss structure contribute to noise radiation and fatigue failure at the welded joint connecting the web and flange plates. Therefore, it is necessary to investigate the instability of local vibrations for the members of a steel truss structure.

Many studies on the problems associated with instability of local vibration of thin-walled members have been performed.

For example, Yamaki and Nagai[1)] investigated the dynamic instability problems of rectangular plates under periodic compressive forces. They clarified that the principal region of instability is of importance when the loading sides are simply supported and that combined resonances are also produced when the loading sides are fixed.

Takahashi and his colleagues[2)-5)] and Kuranishi, Fukaya and Shima[6)] studied the instability of out-of-plane bending vibration in the web of plate girders subjected to periodic bending moment and clarified some of the characteristics. However, they assumed that the horizontal sides of the web plate connecting to flange plates are hinged or fixed. Few reports have been published on the analysis of the instability of local vibration taking into account the coupled vibration of component plates of plate girders.

This study clarifies the characteristics of the instability of local vibrations of thin-walled members under periodic axial forces. Box section and H-section members, which are typical members of a truss structure, are analyzed by using the finite strip method. Firstly, local buckling and free local vibration are analyzed, and their characteristics are investigated. Secondly, the regions of instability of local vibration of the members with various geometrical parameters are calculated and the effects of some factors which control the instability phenomena are clarified. Lastly, based on the results, the most efficient arrangements

This paper is translated into English from the Japanese paper, which originally appeared on J. Struct. Mech. Earthquake Eng., JSCE, No.577/I-41, pp.131-139,1997.10.

of diaphragm or stiffener are discussed.

2. ANALYTICAL METHOD

A typical strip i with nodal lines 1 and 2 is shown in **Fig. 1**. If it is assumed that the longitudinal ends of the strip are hinged, the displacement functions of components, u, v and w, in directions x, y and z are written as

$$\begin{Bmatrix} u \\ v \\ w \end{Bmatrix} = \sum_{m=1}^{r} \begin{bmatrix} \langle N_p \rangle C_m & 0 & 0 \\ 0 & \langle N_p \rangle S_m & 0 \\ 0 & 0 & \langle N_b \rangle S_m \end{bmatrix} \begin{Bmatrix} \{U_{i,m}\} \\ \{V_{i,m}\} \\ \{W_{i,m}\} \end{Bmatrix} \tag{1}$$

where r is the number of terms of series in the longitudinal direction. $\langle N_p \rangle$ and $\langle N_b \rangle$ are shape functions in the transverse direction, which have the form

$$\langle N_p \rangle = \langle 1-\eta \quad \eta \rangle \tag{2}$$

$$\langle N_b \rangle = \langle 1-3\eta^2+2\eta^3 \quad y(1-2\eta+\eta^2) \quad 3\eta^2-2\eta^3 \quad y(\eta^2-\eta) \rangle \tag{3}$$

where $\eta = y/d$, C_m and S_m are the m-th terms of the harmonic functions in the longitudinal direction, which are given by

$$C_m = \cos\left(\frac{m\pi}{L}x\right) \tag{4}$$

$$S_m = \sin\left(\frac{m\pi}{L}x\right) \tag{5}$$

and $\{U_{i,m}\}$, $\{V_{i,m}\}$ and $\{W_{i,m}\}$ are the vectors of nodal line displacements corresponding to the m-th term of longitudinal series, which have the forms

$$\{U_{i,m}(T)\} = \begin{Bmatrix} u_{1,m}(T) \\ u_{2,m}(T) \end{Bmatrix} \tag{6}$$

$$\{V_{i,m}(T)\} = \begin{Bmatrix} v_{1,m}(T) \\ v_{2,m}(T) \end{Bmatrix} \tag{7}$$

$$\{W_{i,m}(T)\} = \begin{Bmatrix} w_{1,m}(T) \\ \theta_{1,m}(T) \\ w_{2,m}(T) \\ \theta_{2,m}(T) \end{Bmatrix} \tag{8}$$

where T is the variable for time.

Substituting the displacement functions of Eq. (1) into the equation of virtual work, the equations of motion for a strip are derived. Transforming the matrices in the local coordinate system for strips into the global coordinate system and rearranging them according to the compatibility of displacements and the equilibriums of forces, the equations of motion for a thin-walled member are obtained.

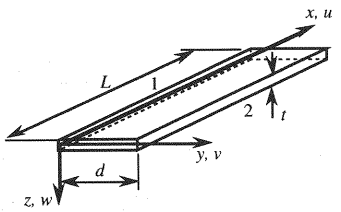

Fig. 1 Finite strip and local coordinates

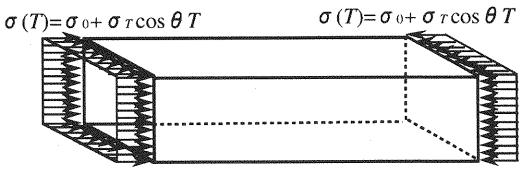

Fig. 2 Thin-walled member subjected to periodic axial stress

When the longitudinal ends are hinged, the equations of motion can be broken down into independent separate equations because of the orthogonal property of the longitudinal series. Therefore, the equation of motion of the m-th term of longitudinal series for the hinged member, which is subjected to uniformly distributed compressive stress shown in **Fig. 2**, is written as

$$[M_m]\{\ddot{d}_m\} + ([K_m] - \sigma_0[K_{Gm}] - \sigma_T \cos\theta T[K_{Gm}])\{d_m\} = \{0\} \tag{9}$$

where σ_0 is the static stress, σ_T is the amplitude of the periodic stress and θ is the circular frequency of the periodic stress. $[M_m]$, $[K_m]$, $[K_{Gm}]$ and $\{d_m\}$ are the mass matrix, stiffness matrix, geometric stiffness matrix and the displacement vector for the m-th term of longitudinal series, respectively.

Setting the periodic stress of Eq.(9) to $\sigma_T = 0$, the eigen equation for free local vibration of the member subjected to the uniformly distributed static stress σ_0 is given by

$$[M_m]\{\ddot{d}_m\} + ([K_m] - \sigma_0[K_{Gm}])\{d_m\} = \{0\} \tag{10}$$

Ignoring the term of inertia and setting the periodic stress in Eq.(9) to $\sigma_T = 0$, the local buckling equation is given by

$$([K_m] - \sigma_0[K_{Gm}])\{d_m\} = \{0\} \tag{11}$$

When the displacement functions of Eqs.(1) are used, the mass matrix $[m_{i,m}]$ and the geometric stiffness matrix $[k_{Gi,m}]$ for the m-th term of longitudinal series for strip i are written as

$$[m_{i,m}]=\begin{bmatrix}[m_{i,m}^{U}] & 0 & 0\\ 0 & [m_{i,m}^{V}] & 0\\ 0 & 0 & [m_{i,m}^{W}]\end{bmatrix} \tag{12}$$

$$[k_{Gi,m}]=\begin{bmatrix}[k_{Gi,m}^{U}] & 0 & 0\\ 0 & [k_{Gi,m}^{V}] & 0\\ 0 & 0 & [k_{Gi,m}^{W}]\end{bmatrix} \tag{13}$$

where,

$$[m_{i,m}^{U}]=\rho t\int_0^L {C_m}^2 dx\int_0^d \langle N_p\rangle\{N_p\}dy \tag{14a}$$

$$[m_{i,m}^{V}]=\rho t\int_0^L {S_m}^2 dx\int_0^d \langle N_p\rangle\{N_p\}dy \tag{14b}$$

$$[m_{i,m}^{W}]=\rho t\int_0^L {S_m}^2 dx\int_0^d \langle N_b\rangle\{N_b\}dy \tag{14c}$$

$$[k_{Gi,m}^{U}]=t\int_0^L \frac{dC_m}{dx}\frac{dC_m}{dx}dx\int_0^d \langle N_p\rangle\{N_p\}dy \tag{15a}$$

$$[k_{Gi,m}^{V}]=t\int_0^L \frac{dS_m}{dx}\frac{dS_m}{dx}dx\int_0^d \langle N_p\rangle\{N_p\}dy \tag{15b}$$

$$[k_{Gi,m}^{W}]=t\int_0^L \frac{dS_m}{dx}\frac{dS_m}{dx}dx\int_0^d \langle N_b\rangle\{N_b\}dy \tag{15c}$$

In Eqs.(14) and (15), the integrations are

$$\int_0^L {C_m}^2 dx=\int_0^L {S_m}^2 dx=\frac{L}{2} \tag{16a}$$

$$\int_0^L \frac{dC_m}{dx}\frac{dC_m}{dx}dx=\int_0^L \frac{dS_m}{dx}\frac{dS_m}{dx}dx=\left(\frac{m\pi}{L}\right)^2\frac{L}{2} \tag{16b}$$

Eqs.(16) produce the result that the mass matrix coincides with the geometric stiffness matrix except for the constant coefficient. Therefore, the local vibration modes derived from Eq.(10) are the same as the local buckling modes derived from Eq.(11), and Eq.(9) can be transformed into the uncoupled equation of motion for each mode by the orthogonal property of the eigen vectors.

Introducing the eigen vector $\{\phi_{m,s}\}$ (s=1, 2, ..., n) and normal coordinate $\xi_{m,s}$, the displacement vector $\{d_m\}$ is written as

$$\{d_m\}=\sum_{s=1}^{n}\{\phi_{m,s}\}\xi_{m,s}=[\Phi_m]\{\Xi_m\} \tag{17}$$

in which

$$[\Phi_m]=\left[\{\phi_{m,1}\}\quad\{\phi_{m,2}\}\quad\cdots\quad\{\phi_{m,n}\}\right]$$

$$\{\Xi_m\}=\langle\xi_{m,1}\quad\xi_{m,2}\quad\cdots\quad\xi_{m,n}\rangle^T$$

By substitution of Eq. (17) into Eq. (9) and front multiplication of Eq.(9) by $[\Phi_m]^T$, the matrices $[M_m]$, $[K_m]$ and $[K_{Gm}]$ are simultaneously transformed into the diagonal form. Then, Eq. (9) is simplified into a series of independent separate equations, each of which depends on the number s of the mode of cross-sectional deformation.

$$\ddot{\xi}_{m,s}+{\omega_{m,s}}^2\left(1-\frac{\sigma_0+\sigma_T\cos\theta T}{\sigma_{m,scr}}\right)\xi_{m,s}=0 \tag{18}$$

where,

$${\omega_{m,s}}^2=\frac{k_{m,s}}{m_{m,s}},\qquad \sigma_{m,scr}=\frac{k_{m,s}}{k_{Gm,s}} \tag{19), (20}$$

$$m_{m,s}=\langle\phi_{m,s}\rangle[M_m]\{\phi_{m,s}\} \tag{21}$$

$$k_{m,s}=\langle\phi_{m,s}\rangle[K_m]\{\phi_{m,s}\} \tag{22}$$

$$k_{Gm,s}=\langle\phi_{m,s}\rangle[K_{Gm}]\{\phi_{m,s}\} \tag{23}$$

Introducing the damping constant $h_{m,s}$ to Eq.(18), authors obtain

$$\ddot{\xi}_{m,s}+2h_{m,s}\omega_{m,s}\dot{\xi}_{m,s}+{\omega_{m,s}}^2\left(1-\frac{\sigma_0+\sigma_T\cos\theta T}{\sigma_{m,scr}}\right)\xi_{m,s}=0 \tag{24}$$

Introducing the natural circular frequency of the member under static stress σ_0

$$\Omega_{m,s}=\omega_{m,s}\sqrt{1-\frac{\sigma_0}{\sigma_{m,scr}}} \tag{25}$$

and the excitation parameter

$$\mu_{m,s}=\frac{1}{2}\cdot\frac{\sigma_T}{\sigma_{m,scr}-\sigma_0} \tag{26}$$

Eq.(24) is rewritten as

$$\ddot{\xi}_{m,s}+2h_{m,s}\omega_{m,s}\dot{\xi}_{m,s}+{\Omega_{m,s}}^2\left(1-2\mu_{m,s}\cos\theta T\right)\xi_{m,s}=0 \tag{27}$$

This is the equation of motion on normal coordinates $\xi_{m,s}$ for the m-th term of longitudinal series and the s-th mode of cross-sectional deformation. Eq.(27) is a well-known Mathieu equation and is the equation of dynamic instability of lateral motion of a bar which was presented by Bolotin[7].

Based on Eq.(27), the equations of boundary frequencies of regions of instability for local vibrations of thin-walled members under periodic axial stress are

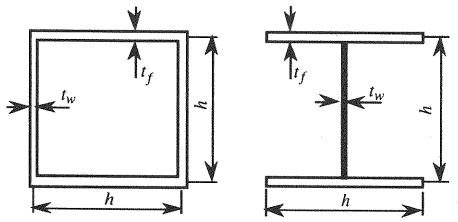

Fig. 3 Models for analyses

derived approximately as follows[7]. principal regions:

$$\theta = 2\Omega_{m,s}\sqrt{1 \pm \sqrt{\mu_{m,s}{}^2 - 4\frac{\omega_{m,s}{}^2 h_{m,s}{}^2}{\Omega_{m,s}{}^2}}} \qquad (28)$$

secondary regions:

$$\theta = \Omega_{m,s}\sqrt{1 - \mu_{m,s}{}^2 \pm \sqrt{\mu_{m,s}{}^4 - 4\frac{\omega_{m,s}{}^2 h_{m,s}{}^2}{\Omega_{m,s}{}^2}\left(1 - \mu_{m,s}{}^2\right)}} \qquad (29)$$

3. CHARACTERISTICS OF LOCAL BUCKLING AND LOCAL VIBRATION

(1) Outline of Analysis

The models used in this study, which are typical cross-sections of the component members of truss structures, are shown in **Fig. 3**. It is assumed that the members are elastic and the longitudinal ends are hinged. The dimensions of the cross-sections and the material values adopted here are as follows:

h=50.0cm, t_f=2.5cm
Young's modulus E=206Gpa
Poisson's ratio ν=0.3
density ρ=7850kg/m^3

To investigate the effect of the difference of plate thickness on the characteristics of local buckling and local vibration, three thickness ratios of web to flange are studied for each cross-sectional shape:

t_w/t_f=0.4, 0.6, 0.8

Flange and web plates of these members are divided into ten strip elements, respectively.

The problems of buckling and free vibration of the members shown in **Fig. 3** are analyzed by using Eqs.(10) and (11), and the characteristics are investigated. Moreover, in order to clarify the effect of coupling of flange and web plates, web plates are modeled into rectangular plates and are analyzed. There are two types of boundary conditions of the rectangular plate: hinged along all edges,; and hinged along the loaded edges and fixed along the other edges.

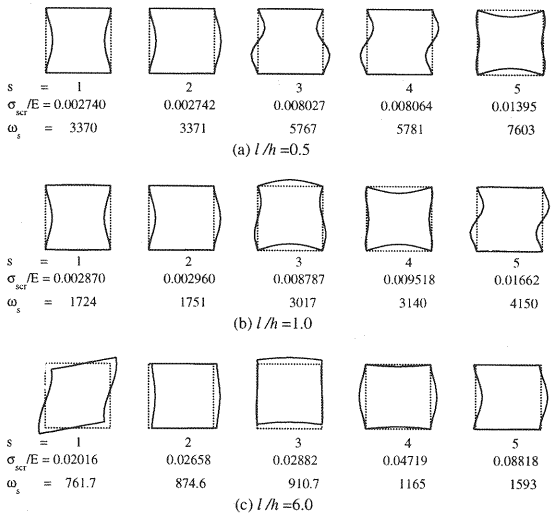

Fig. 4 Mode shapes of buckling and free vibration for box section members (t_w/t_f = 0.4)

For convenience, the analytical results are arranged by using the longitudinal half-wavelength l ($=L/m$) instead of span L and the number m of the longitudinal half-waves of buckling modes or free vibration modes.

(2) Box Section Members

For the box section members, the buckling and free vibration analyses are carried out with varying longitudinal wavelength.

For the case of l/h=0.5, 1.0 and 6.0, the mode shapes of buckling and free vibration of the members with t_w/t_f=0.4 are shown in **Fig. 4**. The buckling stresses and the natural circular frequencies are also shown. As described in Section **2**, the mode shapes of buckling are the same as those of free vibration. As the wavelength increases, the modes change from the out-of-plane deformation of component plates to the overall deformation. Natural circular frequencies decrease as the longitudinal half-wavelength increases. Buckling stresses of the members with l/h=0.5 and 1.0, which are dominated by local deformation, are lower than those of the members with l/h=6.0, which are dominated by overall deformation.

The lowest buckling stresses of the box section members have been calculated with varying longitudinal half-wavelength. The results for the box sections with t_w/t_f=0.4, 0.6 and 0.8 are shown in **Fig. 5** as a series of curves of σ_{cr}/E versus l/h. The ordinate σ_{cr}/E and the abscissa l/h respectively denote the ratio of buckling stress σ_{cr} for Young's modulus E and the longitudinal half-wavelength normalized with the height h of the member, and are indicated on logarithmic scales. The curves for all thickness ratios exhibit the

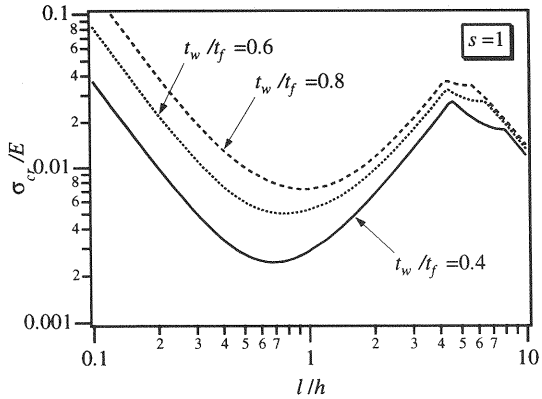

Fig. 5 Buckling stress versus longitudinal half-wavelength for box section members

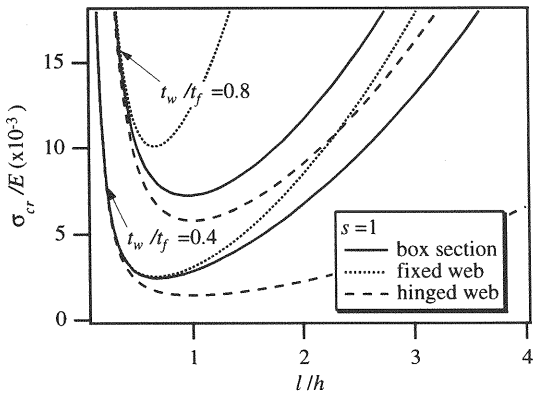

Fig. 6 Comparison of buckling strength for box section member with webs which are modeled as rectangular plates

same tendency, which have a minimum value at *l/h* nearly equal to 1 and a maximum value at *l/h* =4. Referring to **Fig. 4**, it is found that the curves at *l/h* below 4 correspond to the local buckling. As the thickness ratio t_w/t_f decreases, the local buckling stress decreases and *l/h* for minimum local buckling stress decreases.

Figure 6 compares the lowest buckling stresses for the box section members with those of the webs which are modeled as rectangular plates. The curves for the thickness ratio t_w/t_f=0.4 and 0.8 are shown there. The rectangular plates have two types of boundary conditions: hinged along all edges,; and hinged along the loaded edges and fixed along the other edges. The curves of the box section members at *l/h* under 0.4 approximately agree with those of the webs and the difference of the buckling stress between the box section member and the web increases as *l/h* increases. The range of *l/h* where the buckling stress is almost the same as those of webs becomes narrow as t_w/t_f increases. The minimum buckling stress for the box section member with t_w/t_f=0.4 approximately coincides with that for the fixed web and the minimum buckling

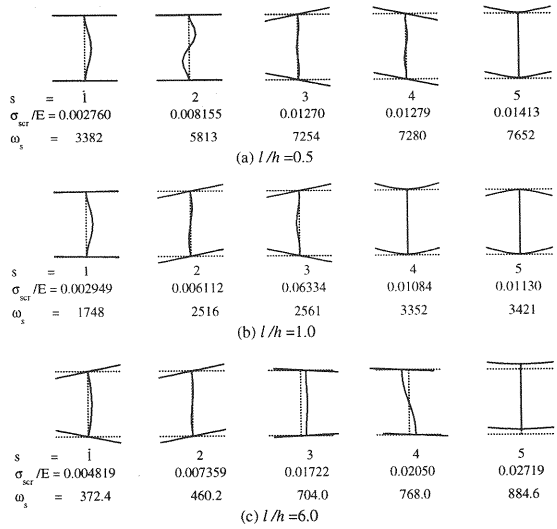

Fig. 7 Mode shapes of buckling and free vibration for H-section members (t_w/t_f = 0.4)

stress for the box section member with t_w/t_f=0.8 is approximated to that for the hinged web.

(3) H-Section Members

In the same way as the box section members, buckling and free vibration analyses for the H-section members are carried out. Some of the results are shown in **Fig. 7-9**.

Figure 7 shows the mode shapes of buckling and free vibration for the members with t_w/t_f=0.4 for the case of *l/h*=0.5, 1.0 and 6.0. Some of the mode shapes of *l/h*=0.5 and 1.0 are predominated by local deformation of the web or flange. Mode shapes of *l/h*=6.0 show the coupled deformation of web and flange. These results show that the mode shapes change from local deformation to overall deformation as *l/h* increases.

The relations between the lowest buckling stress and *l/h* are shown in **Fig. 8**. The curves have different tendencies depending on the value of t_w/t_f and the curve of t_w/t_f=0.8 has a minimum value at *l/h*=1.7. Referring to **Fig. 7**, it is found that the mode shapes for the lowest buckling stress of the H-section member change from web buckling to coupled buckling of component plates as *l/h* increases. Moreover, it is estimated that the mode shapes for the minimum local buckling stress change from web buckling to coupled buckling of flanges and web as t_w/t_f increases.

Figure 9 compares the lowest buckling stress for the H-section members with those of the webs which are modeled as rectangular plates. The rectangular plates have two types of boundary conditions which are also used in **Fig. 6**. In the range where *l/h* is small, the buckling curves of the H-section member approximately agree with those of the webs. The minimum

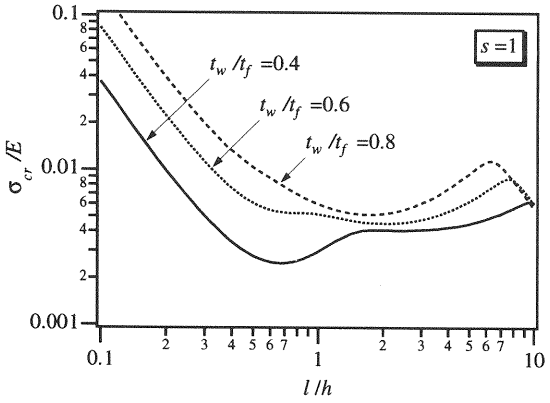

Fig. 8 Buckling stress versus longitudinal half-wavelength for H-section members

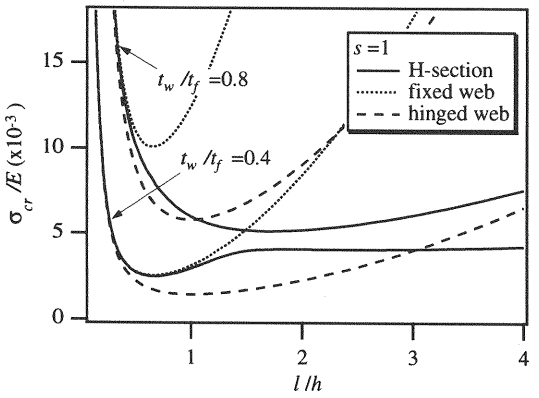

Fig. 9 Comparison of buckling strength of H-section members with the webs which are modeled as rectangular plates

value of the member with t_w/t_f=0.4 coincides with those of the fixed web. The minimum value of the H-section member with t_w/t_f=0.8 is less than that of the hinged web. It is found that the minimum buckling stress of the H-section member with t_w/t_f=0.8 depends on the coupled buckling of component plates.

4. CHARACTERISTICS OF INSTABILITY OF LOCAL VIBRATION

In this section, the characteristics of instability of local vibration for the models illustrated in **Fig. 3** will be described. Based on the results, the period of periodic force which easily yields dynamic instability and the most efficient arrangements of diaphragm or stiffener will be investigated.

Referring to Section **2**, the boundary frequencies of principal and secondary regions of instability for the *m*-th x *s*-th mode are determined by Eq.(28) and (29), where *m* and *s* respectively mean the number of terms of longitudinal series and the number of modes of

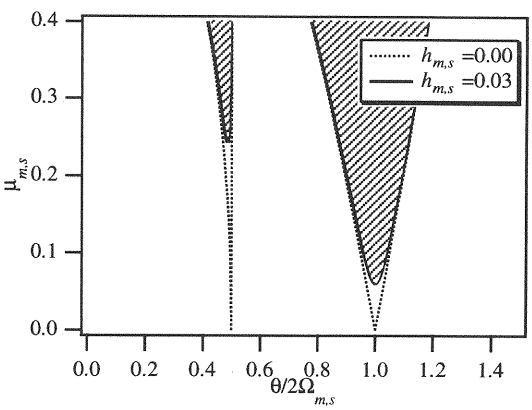

Fig. 10 Regions of dynamic instability

cross-sectional deformation. The result is shown in **Fig. 10**. The ordinate $\mu_{m,s}$ denotes the excitation parameter and θ and $\Omega_{m,s}$ of the abscissa respectively denote the circular frequency of the periodic stress and the natural circular frequency of the *m*-th x *s*-th mode for the member. The solid lines and the dotted lines respectively denote the boundary frequencies for damping constant $h_{m,s}$= 0.03 and 0.00 and the cross-hatched area denote the regions of instability for $h_{m,s}$=0.03.

This is the well-known graph of regions of instability for simple parametric resonances. As shown in Section **2**, the regions of instability for each local vibration can be illustrated as shown in **Fig. 10** by using the non-dimensional ordinate and abscissa for the case where the mode shapes of free vibration for the member are the same as those of buckling. This property does not depend on the shape and dimensions of a cross-section nor the order of local vibration mode.

Although **Fig. 10** shows the regions of instability for each local vibration mode, it does not present the differences in the characteristics of instability among them. Thus, authors clarify them by comparing the changes of the regions of instability with the longitudinal half-wavelength for the cases where the number of modes of cross-sectional deformation and the loading conditions are fixed.

Figure 11 shows the changes of the principal regions of instability for the first mode of cross-sectional deformation with the number of longitudinal half-waves. The conditions of the members are as follows: L/h=5.0, σ_0=0.0, σ_T/E =0.001 and $h_{m,s}$=0.0. The *l*/*h* of the abscissa denotes the longitudinal half-wavelength (=L/m) normalized with the height of the members. The marks ●, ■, ▲ respectively denote the boundary frequencies of the regions for the members with t_w/t_f=0.4, 0.6 and 0.8, and the widths between the two same marks plotted on the same longitudinal half-wavelength show the regions of instability.

The values of *l*/*h* at the widest regions of instability

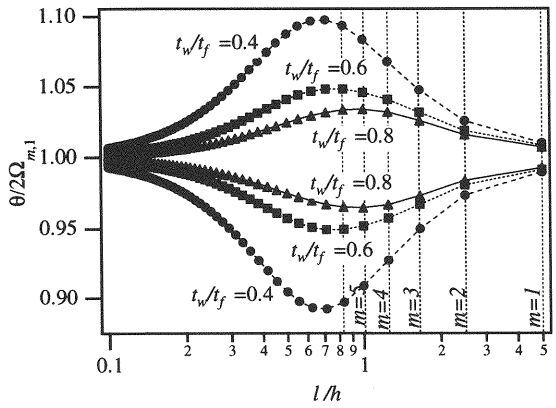

(a) Box section members

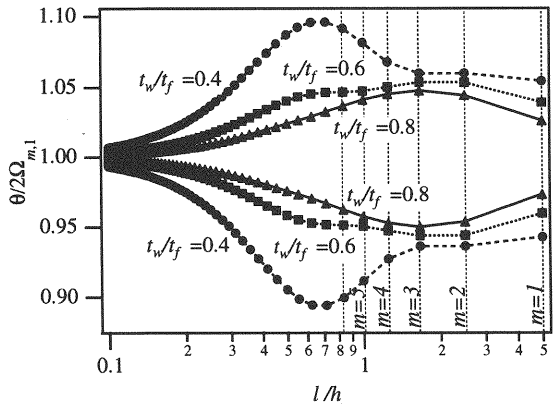

(b) H-section members

Fig. 11 Change of principal regions of instability with number of longitudinal half-waves (L/h=5.0, σ_T/E=0.001, σ_0=0.0, $h_{m,s}$=0.0)

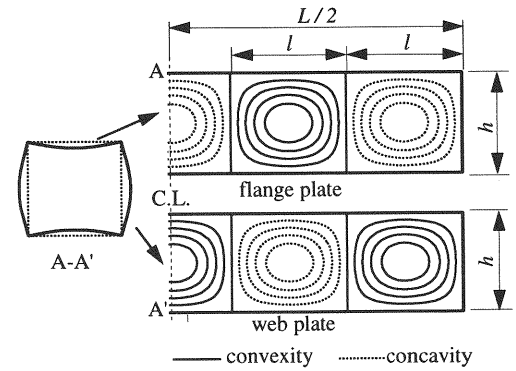

Fig. 12 Mode shape of vibration for box section member at the widest region of instability (t_w/t_f= 0.8, σ_T/E = 0.001, σ_0= 0.0)

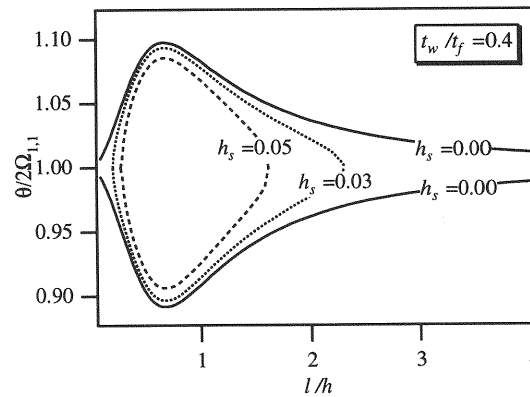

Fig. 13 Effect of damping on principal regions of instability for box section member

for the box section members are under 1.0 (m>5). However, for H-section members, they change from 0.7 to 2.0 with the value of t_w/t_f. By comparing **Fig. 11** with **Figs. 5** and **8**, it is found that the width of the regions of instability increases as the buckling stress decreases.

In **Fig. 11**, the width of the region of instability denotes the range of circular frequency of the axial force which causes parametric resonance vibration. Local vibration easily occurs at the longitudinal half-wavelength at which the region of instability is wide. Therefore, it is possible to control the occurrence of local vibrations by considering these values when the arrangement of the diaphragms and stiffeners is determined.

Figure 12 shows the mode shape of vibration for the box section member with t_w/t_f=0.8 at the widest region of instability illustrated in **Fig. 11(a)**. There are out-of-plane deformations for each component plate and five half-waves along the longitudinal direction.

Figure 13 shows the effects of damping on the principal region of instability for the box section member with t_w/t_f=0.4, σ_0=0 and σ_T/E =0.001. The areas surrounded by the same lines denote the region of instability. The ranges of circular frequency of axial force and longitudinal half-wavelength for the regions of instability narrow as the damping constant increases.

In order to clarify the effect of coupling vibration of component plates, the instability of the web plate modeled as a rectangular plate is investigated and compared with results for the members. **Figure 14** compares the regions of instability for the web plates with those of the box section and the H-section members with t_w/t_f=0.8. The members are subjected to static stress σ_0=0 and periodic stress σ_T/E =0.002. The boundary conditions of the web plates are as given in Section **3**. It is assumed that the mode number of cross-sectional deformation s is equal to 1 and the damping constant $h_{1,1}$ is equal to 0.0.

The boundary frequencies of the web plates agree with those of the members at l/h under 0.5. Especially, for the H-section member, the maximum width of the region of instability is wider than that of the

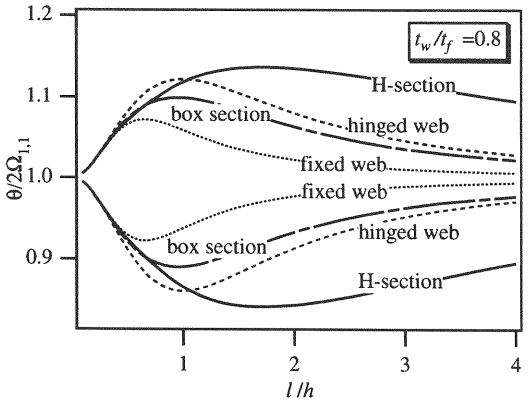

Fig. 14 Comparison of instability regions for members with web plates ($\sigma_T/E = 0.002$, $\sigma_0 = 0.0$, $h_{1,1} = 0.0$)

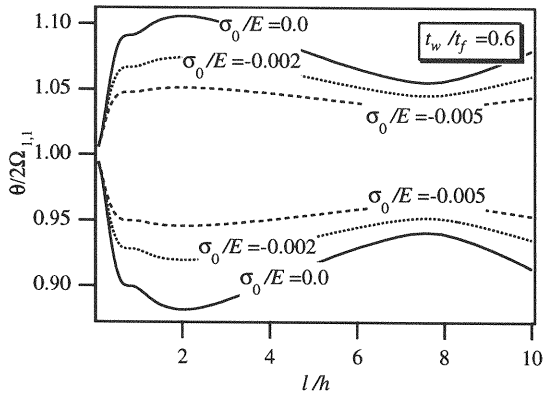

Fig. 15 Effects of static stress on principal instability regions for H-section member ($\sigma_T/E = 0.002$, $h_{1,1} = 0.0$)

hinged web and the longitudinal half-wavelength of the widest region of instability is longer than that of the hinged web. These properties are the same as the results shown in **Figs. 6** and **9**. These results show that the conventional estimations of the regions of instability for the web plate, for which the boundary conditions of the edges joined to the flange are assumed to be simply supported or fixed, are not valid and it is necessary to study the instability of local vibration for the members by considering coupling vibration.

In truss structures, H-section members are used as the tensile members. Therefore, the effect of static stress on their regions of instability is investigated. **Figure 15** shows the regions of instability for the H-section members with t_w/t_f=0.6 for the case where the periodic stress σ_T/E =0.002 and variable static stress (σ_0/E=0.000, −0.002, −0.005) are applied. The regions of instability narrow and are independent of the longitudinal half-wavelength as the static tensile stress increases. Moreover, they yield even if the sum of the static and periodic stress is tensile stress.

5. CONCLUSION

The instability of local vibration of the hinged box section and H-section members was investigated by applying the finite strip method in order to clarify the instability of the members of a truss structure under periodic axial forces. Firstly, local buckling and free vibration of the members, which are fundamental factors of dynamic instability, were analyzed and the characteristics were discussed. In addition, the regions of instability of local vibration for the members under various geometrical parameters were calculated and the effects of some factors which control the dynamic instability phenomena were clarified. The following conclusions were drawn.

1) The mode shapes for the buckling and the free vibration are the same and the equations of motion for dynamic instability for all modes can be rewritten as a Mathieu equation. Therefore, the instability regions for the local vibrations can be shown in the same figure by using suitable non-dimensional ordinate and abscissa. This property is independent of the shape and dimensions of the cross-section and the order of local vibration mode.

2) The region of instability of local vibration is the widest at the mode which has the minimum local buckling strength. For box section members, the regions of instability for the local vibrations become wider at l/h between 0.7 to 1.0. For H-section members, they depend on the plate thickness ratio and have the maximum value at l/h over 1.7 in case of the member with t_w/t_f over 0.6.

3) The analysis of dynamic instability of the web plate modeled as a rectangular plate is adequate for approximating the region of instability of local vibration for the members at l/h under 0.5. The region of dynamic instability of the hinged web is overestimated for box section members and is underestimated for H-section members.

REFERENCES

1) Yamaki, N. and Nagai, K.: Dynamic Stability of Rectangular Plates under Periodic Compressive Forces, *Reports of the Institute of High Speed Mechanics*, Tohoku University, Vol.36, No.351, pp.147-168. 1975 (in Japanese).

2) Takahashi, K., Tagawa, M., Ikeda, T. and Matsukawa, T.: Dynamic Stability of Rectangular Plate Subjected to Inplane Forcing, *Proc. of JSCE*, No.341, pp.179-186, 1984 (in Japanese).

3) Takahashi, K., Konishi, Y., Ikeda, T. and Kawano, R.: Nonlinear Response of a Rectangular Plate Subjected to Inplane Dynamic Moment, *Proc. of JSCE*, No.374/I-6, pp.79-87, Oct. 1986.

4) Takahashi, K., Konishi, Y. and Kawano, R.: Nonlinear Re-

sponse of a Rectangular Plate Subjected to Inplane Moment, *Journal of Structural Eng.*, Vol.32A, pp.705-714, 1986 (in Japanese).

5) Takahashi, K., Konishi, Y., Kawano, R. and Urakawa, S.: Dynamic Stability of Deflected Rectangular Plate under Inplane Dynamic Moment, *Journal of Structural Eng.*, Vol.33A, pp.485-494, 1987 (in Japanese).

6) Kuranishi, S., Fukaya, S. and Shima, T.: Vibration of an Initially Deflected Web Plate under Periodic Beam Bending, *Proc. of JSCE*, No.341, pp.229-232, 1984.

7) Bolotin, V. V.: *Dynamic Stability of Elastic System*, Holden Day Inc., 1964.

8) Brown, J. E., Hutt, J. M. and Salama, A. E.: Finite Element Solution to Dynamic Stability of Bars, *AIAA Journal*, Vol.6, pp.1423-1425, 1968.

9) Hutt, J. M. and Salam, A. E.: Dynamic Stability of Plates by Finite Elements, *Journal of the Engineering Mechanics Division, ASCE*, Vol.97, EM3, pp.879-899, 1971.

10) Ohkoshi, Y., Mikami,T. and Yoshimura, H.: Dynamic Instability of I-section Members under Periodic Loads, *Proc. of the 38th Annual Conference of JSCE*, pp.178-179, 1983 (in Japanese).